

# Ab Initio QM/MM Free Energy Simulations of Peptide Bond Formation in the Ribosome Support an Eight-Membered Ring Reaction Mechanism

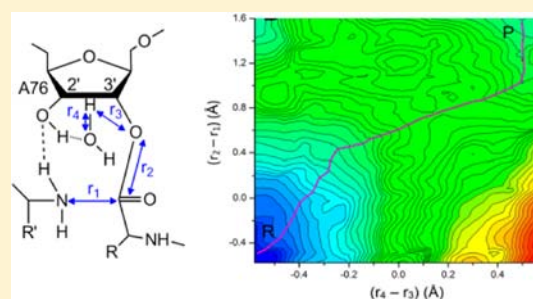
Jun Xu,<sup>†</sup> John Z. H. Zhang,<sup>†,‡</sup> and Yun Xiang<sup>\*,†</sup>

<sup>†</sup>State Key Laboratory of Precision Spectroscopy, Institute of Theoretical and Computational Science, Department of Physics, East China Normal University, Shanghai 200062, China

<sup>‡</sup>Department of Chemistry, New York University, New York, New York 10003, United States

**S** Supporting Information

**ABSTRACT:** *Ab initio* QM/MM free-energy simulations were carried out to study the peptide bond formation reaction in the peptidyl transferase center of the ribosome. The QM part of the reaction was treated by density functional theory at the B3LYP/6-31G\* level, while the MM part including the solvent and RNA environment was described by molecular force field. The calculated free-energy surfaces for the two popular reaction mechanisms, the six- and eight-membered ring reactions, exhibited large energetic differences which favor the eight-membered reaction mechanism. The simulated quasi-transition state structures clearly indicated a “late” feature consistent with previous theoretical studies. Also the important functional role played by water molecules in the active site of the ribosome and its implication in ribozymic catalysis was discussed in detail.



## INTRODUCTION

The peptide bond formation reaction during protein synthesis takes place in the peptidyl transferase center (PTC) of the ribosome.<sup>1,2</sup> This aminolysis reaction commences when the  $\alpha$ -amino group of the aminoacyl-tRNA in the ribosome A-site attacks the ester carbon of the peptidyl-tRNA in the adjacent P-site. After the nitrogen-carbon bond forms, the aminoacyl-tRNA is elongated by one amino acid in the A-site. In recent years, extensive studies including high-resolution crystal structures of the ribosomal 50S unit,<sup>3–6</sup> kinetic measurements,<sup>7–16</sup> biochemical mutagenesis,<sup>11,17–21</sup> and computer simulations<sup>22–27</sup> have been focused on elucidating the chemical basis of the peptide bond formation reaction. The current reaction model points to a substrate-assisted mechanism in which the indispensable 2'-OH group of the P-site RNA residue A76 plays an important role in mediating the proton transfer between the attacking nucleophile amino group and the leaving 3' ester group,<sup>6,23,28–30</sup> while other ribosomal groups do not actively participate during the reaction.<sup>11,17,18,20,31,32</sup> Also observed is the hydrogen bonding between the A2451 2'-OH group and A76 2'-OH that may help position and stabilize the substrate.<sup>21</sup> However, a detailed understanding of the peptide-bond formation process and the proton transfer route from  $\alpha$ -amino group in the A-site to the P-site substrate is still lacking.

On the basis of the ribosome active site structure, several possible reaction pathways have been proposed to gain insight into the proton transfer process and among them two are especially popular. One is a six-membered ring mechanism in which proton is transferred via the 2'-OH group of the P-site

A76<sup>28</sup> (see Figure 1). The other one is an eight-membered mechanism in which an additional water molecule acts as a bridge between the 2'-OH group and 3'O of P-site A76 for proton transfer<sup>6</sup> (see Figure 1). Early studies by Aqvist and co-workers<sup>23</sup> using empirical valence bond (EVB) potential combined with classic molecule dynamics (MD) simulations on the six-membered mechanism yielded a reaction barrier in agreement with experimental data. Furthermore, Warshel and co-workers performed *ab initio* calculations with Langevin dipole (LD) solvent model to scan the six-membered reaction energy surfaces for a model reaction in water.<sup>22</sup> Steitz et al. proposed the eight-membered reaction mechanism based on the high-resolution crystal structures in which a water molecule was found to be in close contact with both the 2'O and 3'O groups of the P-site A76.<sup>6</sup> Actually, in previous MD simulations, Aqvist and co-workers predicted the presence of this additional water and also a preorganized hydrogen bond network that may stabilize the reaction in the PTC.<sup>23,24</sup> They further investigated the eight-membered mechanism by using *ab initio* quantum calculations of the reaction potential energy surface for a 76-atom ribosomal active site model, and their computational results seemed agree with experimental energetics.<sup>26</sup> Here, the questions have been narrowed down to: which mechanism is more favorable for the protein synthesis reaction in the ribosome?

Received: August 2, 2012

Published: September 6, 2012

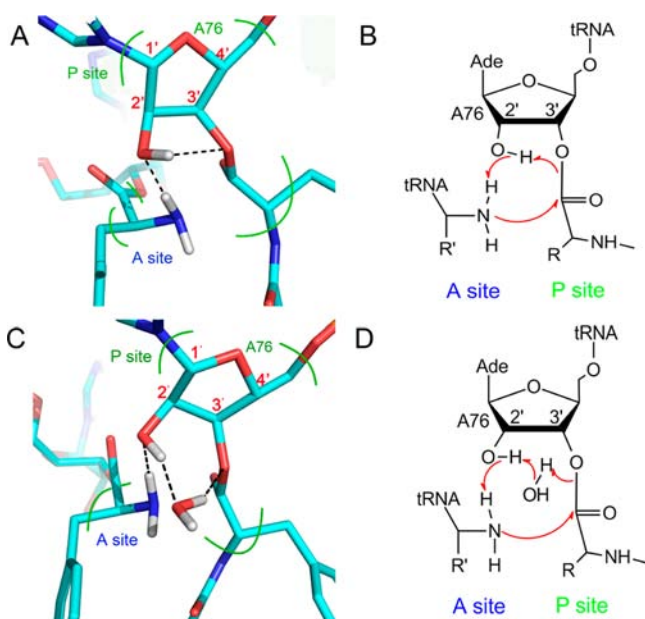


**Figure 1.** (A and B) Six-membered ring reaction mechanism: a proton shuttle via 2'-hydroxyl in the P site. (C and D) Eight-membered ring reaction mechanism: a water molecule, interacting with the 2'- and 3'-hydroxyls of A76 in the P site, acts as a proton relay. The green curves in panels A and C indicate the QM/MM boundaries.

Proton transfer is ubiquitous in chemical and biological reaction systems. Many complex reaction processes are usually initiated or accompanied by proton transfer events, such as in serine proteases and DNA polymerases, to name but a few. Because of its high dynamic mobility and hydrogen-bonding versatility, the participation of water in proton transfer reactions makes the elucidation of enzymatic reaction mechanism a complicated and challenging issue which is not fully resolved for many enzyme systems. The transient nature of the reaction intermediate and transition state also causes paramount difficulty in capturing these structures by experimental means. The utilization of transition state analogues offers tremendous help but could be misleading if the results were not interpreted properly.

In this work, we address these questions by performing extensive free energy simulations using a hybrid *ab initio* quantum mechanical/molecular mechanical (QM/MM) potential.<sup>33–43</sup> In the QM/MM simulation of the peptide bond formation reaction in the ribosome, key residues and substrate atoms in the active site of PTC directly involved in the formation of the C–N bond are treated by density functional theory (DFT), while the surrounding environment including the RNA, ions and solvent water molecules is described by the molecular force field. This QM/MM scheme, which combines the accuracy of QM methods and the efficiency of MM methods, is then exploited in the MD simulation of the free energy profiles of the six-membered and eight-membered reactions. The simulated two-dimensional reaction free-energy surfaces allow us to carry out a detailed analysis and thorough examination of the validity of these two proposed mechanisms. The simulated reaction free-energy differences provide us with a definite and quantitative criterion to discriminate these mechanistic proposals and may eventually help us figure out what is really happening in the ribosome active site. Also the structural features revealed in the simulations help us gain deep insight into the nature of the reaction transition state (TS).

We need to clarify at this point that in this work we are focusing on elucidating the reaction mechanism of the peptide bond formation, rather than on the catalytic factors that make the reaction faster ( $10^7$ -fold rate enhancement measured experimentally) in the ribosome than in water, even though these two important issues are intimately related. The issue about the catalytic mechanism of ribosome was discussed in a previous study<sup>22</sup> where a six-membered ring reaction scheme was assumed.

## METHODS AND SIMULATION DETAILS

The QM/MM model was prepared by selecting all residues with atoms within 30 Å radius of the reaction center (PDB ID: 1VQP). Then, the system was solvated in a 22 Å water sphere which was also centered on the reaction region. The surface-constrained all atom solvent model<sup>44</sup> was used. The resulting QM/MM systems consisted of a QM part of 26 atoms and 5594 atoms in the MM part for the six-membered reaction, and a QM part of 29 atoms and 5552 atoms in the MM part for the eight-membered reaction. The long-range electrostatic effect among RNA and solvent were treated with a local reaction field.<sup>45</sup> The detailed QM/MM partition for the six-membered mechanism and eight-membered mechanism is shown in Figure 1. The QM region includes the A76 ribose moiety, the 2'-hydroxyl group, the 3'-ester group and the  $\alpha$ -amino group. An extra water molecule was added to the QM region in the eight-membered reaction simulation. The QM/MM boundary was chosen to be A76 1' carbon–nitrogen bond, A76 4' carbon–carbon bond, A76 3' ester carbonyl carbon–carbon bond and two carbon–carbon bonds of the  $\alpha$ -amino group (see Figure 1). Six hydrogen link atoms were added to the QM part when *ab initio* QM calculation was carried out. The partial charges of the link atoms were redistributed to all the QM atoms when the electrostatic energy between QM and MM part was calculated by Coulomb interaction. Atoms in the MM part were described by the molecular force field in MOLARIS.<sup>46</sup> A 15 Å cutoff was used for both electrostatic and van der Waals interactions. The QM energy was calculated using the GAUSSIAN 09 software package,<sup>47</sup> with the B3LYP density functional<sup>48,49</sup> and the 6-31G\* basis set. The MD simulation was carried out by the MOLARIS program, and a computer script<sup>50</sup> was used to bridge these two programs. For detailed calculation procedure about how this script works to call the GAUSSIAN program and the MOLARIS program in the MD simulation, see Xiang et al.<sup>50</sup>

Before the QM/MM simulations, both reaction structure models were fully relaxed by running regular MD simulation for 200 ps. The root mean squared deviation (rmsd) between the relaxed structure and the starting crystal structure is 0.9 Å. As previous studies indicate that both six-membered and eight-membered reaction mechanisms are concerted rather than stepwise,<sup>26</sup> here we chose a set of relatively simplified reaction coordinates to depict the reaction free energy landscape in order to reduce the computational time in treating this multidimensional free energy simulation problem. The resulting two-dimensional reaction coordinates for the six-membered reaction were chosen to be  $R_1 = R_{\text{H}_2\text{O}} - R_{3'\text{OH}}$  ( $r_4 - r_3$  in Figure 2A) and  $R_2 = R_{\text{CO}} - R_{\text{NC}}$  ( $r_2 - r_1$  in Figure 2A), where  $R_{\text{NC}}$  denotes the distance between the attacking amine nitrogen and the 3' ester carbonyl carbon,  $R_{\text{CO}}$  the distance between the 3' ester carbonyl carbon and 3' oxygen atom,  $R_{\text{H}_2\text{O}}$  the distance between 2'O and its leaving proton, and  $R_{3'\text{OH}}$  the distance between the leaving proton and its acceptor 3'O. Similarly, for the eight-membered reaction, we used the same  $R_2$  reaction coordinate ( $r_2 - r_1$  in Figure 2B), but  $R_1$  was set to be  $R_1 = R_{\text{OH}} - R_{\text{H}_3'\text{O}}$  ( $r_4 - r_3$  in Figure 2B), where  $R_{\text{OH}}$  is the distance between the oxygen atom of the water molecule (which is absent in the six-membered reaction model) and the transferring proton on water, and  $R_{\text{H}_3'\text{O}}$  is the distance between this leaving proton and its acceptor 3'O. This reaction coordinate setup mainly characterizes the process that the nitrogen atom attacks the ester carbonyl carbon to form the peptide bond and the 3'-oxygen obtains a proton to form the ribose 3'-hydroxyl group.

The *ab initio* QM/MM MD simulations were carried out at 310 K. A total of 90 umbrella sampling windows were used for the simulations

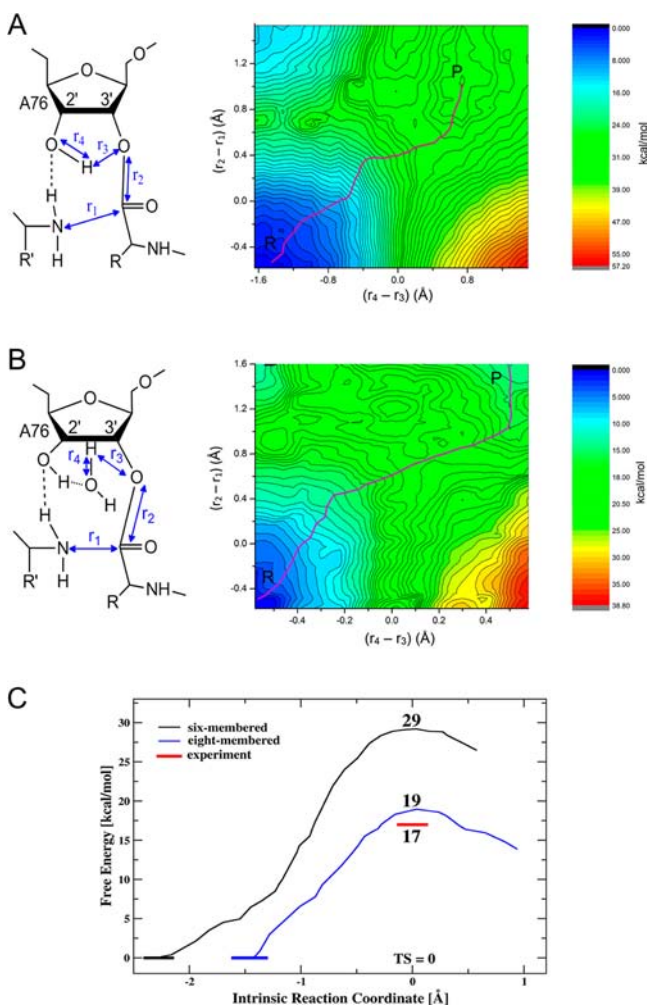


**Figure 2.** (A) The simulated two-dimensional free-energy surface of the six-membered reaction.  $r_4 - r_3$  represents  $2'\text{O}-\text{H}$  distance minus  $\text{H}-3'\text{O}$  distance;  $r_2 - r_1$  represents  $3'\text{O}-\text{C}$  distance minus  $\text{C}-\text{N}$  distance. (B) The simulated two-dimensional free-energy surface of the eight-membered reaction.  $r_4 - r_3$  represents  $\text{H}-\text{O}$  (water) distance minus  $\text{H}-3'\text{O}$  distance;  $r_2 - r_1$  represents  $3'\text{O}-\text{C}$  distance minus  $\text{C}-\text{N}$  distance. (C) The minimum free-energy paths along the intrinsic reaction coordinate for the (A) six- and (B) eight-membered mechanisms. Experimental reaction barrier is also labeled in the graph for comparison.

of the eight-membered reaction, while 107 windows were employed for the six-membered reaction. In each window, the atoms in the reaction coordinates were constrained by harmonic potentials with force constants of varied strength. Apart from these atoms directly involved in peptide bond formation, other hydrogen atoms involved in the proton transfer (hydrogen atom on amino group, hydrogen atom on  $2'\text{O}$  in the eight-membered mechanism) were constrained by using a very small harmonic potential to ensure that these protons would not drift away from their donor–acceptor partners. In each simulation window, the system was first relaxed for 10 ps, and then the production run lasted for 10 ps, with a time step of 1 fs. The probability distributions under different biased windows were pieced together by using the weighted histogram analysis method.<sup>51</sup> After the free-energy profiles for both six-membered and eight-membered reactions were obtained, a detailed comparison of the simulated energetics and structures between these two mechanisms was performed.

## RESULTS AND DISCUSSION

The mechanism of the peptidyl transferase reaction in the ribosome has become a central focus of current ribosomal studies. Especially controversial is the proton transfer process concerning how many protons are in motion and their itinerary during reaction. Regarding this issue, we believe the final judge may be provided by computational free energy simulations, of course, complemented by experimental crystallographic and biochemical studies. A major difference, or advancement, between the current work and previous theoretical studies involving quantum chemical calculations is that we explore the free energy landscape of the reaction while explicitly taking the large ribosome environment into account in our simulations. Previous theoretical works involving quantum chemical calculations inevitably used small reaction models and unfortunately neglected the important RNA/solvent environmental effects that could have major impact on the reaction in the ribosome. Also the energies they obtained were reaction enthalpies, and thus, the entropic component was missing. Enthalpy–entropy decomposition is computationally less reliable because entropy calculation requires extensive sampling.

**Free-Energy Surface.** The simulated two-dimensional free-energy surfaces for the six- and eight-membered reaction were shown in Figure 2 for comparison. As seen clearly from these figures, the calculated free-energy barrier of the eight-membered mechanism, 19 kcal/mol, is in quantitative agreement with the experimental result of 16.5 kcal/mol,<sup>10,14</sup> while, on the contrary, the reaction barrier for the six-membered mechanism is 10 kcal/mol higher than that of the eight-membered reaction. Although because of the simplified reaction coordinate that we used in the calculations this reaction pathway does not exactly represent the complete reaction process from reactant to product, it still faithfully reproduces the C–N bond formation process and the protonation of the ribose  $3'\text{O}$  group. Previous quantum chemical studies on searching for the six-membered transition state with implicit solvent model resulted in much higher reaction barrier.<sup>22,26</sup> In our present study using computational scans of the six-membered reaction path, the simulation, which included explicitly the solvent and RNA environment, also led to quite large energy barrier. Thus, our results indicate that the eight-membered mechanism is much more probable for the ribosomal peptide bond formation reaction.

An important feature to note is that, on Figure 2A,B, the  $x$ -axis, that is, the  $R_1$  coordinate, has very different length range, and is much larger for the six-membered reaction (Figure 2A). This means that in this case the proton has to travel longer distance from the donor to the acceptor to complete the transfer. This is associated with large strain energy penalty, which explains why the free energy barrier for the six-membered reaction is much higher than that of the eight-membered one. With the help of one water molecule, the proton transfer is much easier. Regarding the calculated free energies corresponding to the two reaction mechanisms, we believe it is appropriate and instructive to take a probability view. What is exactly happening in the ribosome active site certainly depends on the availability of water molecules.

**Quasi-Transition State Structure.** On the basis of the two-dimensional free-energy surfaces obtained from QM/MM MD simulations, the transition state structures (or more precisely, transition state ensemble) corresponding to the two

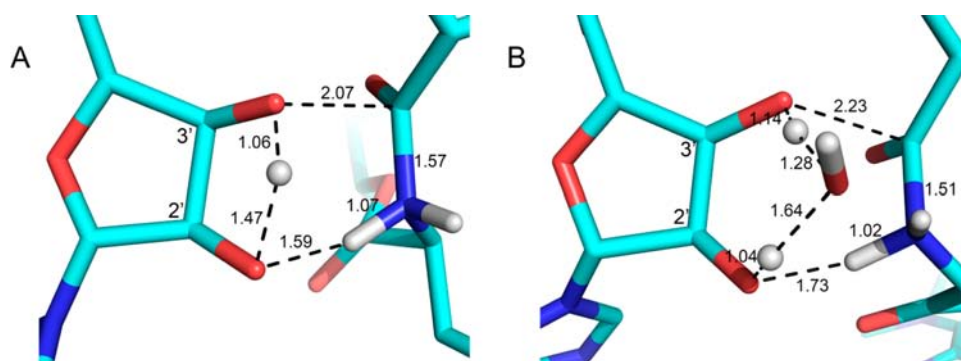


**Figure 3.** (A) Simulated TS structure of the six-membered reaction mechanism. (B) Simulated TS structure of the eight-membered mechanism. Atom distances are in angstroms (Å).

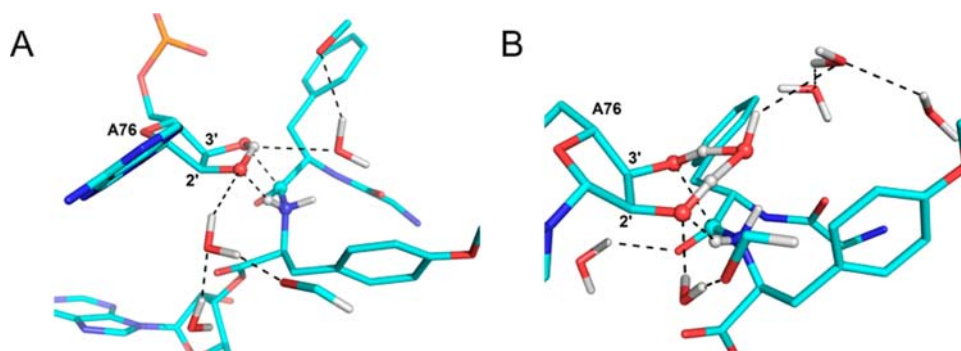


**Figure 4.** Hydrogen bond network in the ribosome active site for the six-membered reaction (A) and for the eight-membered reaction (B).

reaction mechanisms can then be identified and are shown in Figure 3. Inspecting these structures, it is evident that both the six- and eight-membered reactions presented a “late”<sup>26</sup> transition state for the peptidyl transfer reaction that the C–O bond cleavage takes place after the C–N bond formation. In the six-membered reaction TS, C–O ester bond distance reached 2.07 Å and the C–N bond length is 1.57 Å, while the eight-membered TS formed with C–O bond distance of 2.23 Å and C–N bond distance of 1.51 Å. Such TS was formed with the stretch of the ester C–O bond, while the C–N bond formation was almost completed. Previous *ab initio* QM scan in water with partially relaxed geometry suggested a similar late transition state.<sup>22</sup> Our results generally agree with these studies, but show subtle differences in terms of bond length. This is to be expected since our calculations are performed with the ribosome environment included.

In addition, in the six-membered TS, the distance between the transferring proton and 3'O was 1.06 Å, which is slightly closer than that in the eight-membered TS. With the help of one water molecule, it is easier for the proton to transfer over to 3'O in the eight-membered mechanism than in the six-membered mechanism. However, here we did not include the other proton transfer process in the free-energy surface scan. Therefore, we can term these structures as “quasi-transition state”. The precise positions of the transferring protons in the TS structures may change when more degrees of freedom are considered in the reaction coordinate. Thus, more detailed work needs to be done in subsequent research to further investigate this problem. But of course, that will increase the computational cost significantly.

**Hydrogen Bond Network.** To further illustrate the structural elements that may contribute to the reaction transition state stabilization, we plotted the hydrogen bond

network around the ribosome active site. As shown in Figure 4, for both simulated reactions, there are multiple water molecules in the active site forming hydrogen bond with the substrate and RNA residues. In the six-membered mechanism (Figure 4A), a water molecule hydrogen bonded to 2'O to stabilize the 2'O in the TS<sup>22–24,26</sup> and this water molecule was further hydrogen bonded to another water molecule and an A residue. There is a third water molecule near a hydrogen atom of the amino group (Figure 4A) that formed hydrogen bonds with the amine and a C residue. In the eight-membered reaction (Figure 4B), a water molecule near 2'O was also found to be hydrogen bonded with 2'O and an A residue. A hydrogen atom of the water molecule involved in the active site was in close contact with a water molecule, and there are three water molecules which formed a hydrogen bond network (Figure 4B). In addition to those mentioned above, a water molecule that made hydrogen-bonding contacts with the oxyanion in the A site was found in the eight-membered mechanism scan. This water contributes to the TS charge stabilization of the oxyanion during peptide bond formation.<sup>52</sup> As we did not spot a water molecule in the six-membered reaction simulations in the same position, this water unique for the eight-membered reaction may play an important role in lowering the energy barrier. Besides these hydrogen bonds formed with water molecules, we also observed that the hydrogen bonding between the A2451 2'OH group and A76 2'O is persistently retained during the simulations (not explicitly shown in the figures). Taken together with the simulated energetics detailed above, it is reasonable to conclude that the preorganized hydrogen bond network involving multiple water molecules provides a major source of stabilization of the peptide bond formation reaction on the ribosome.<sup>22–26</sup> Also our simulation results are consistent with

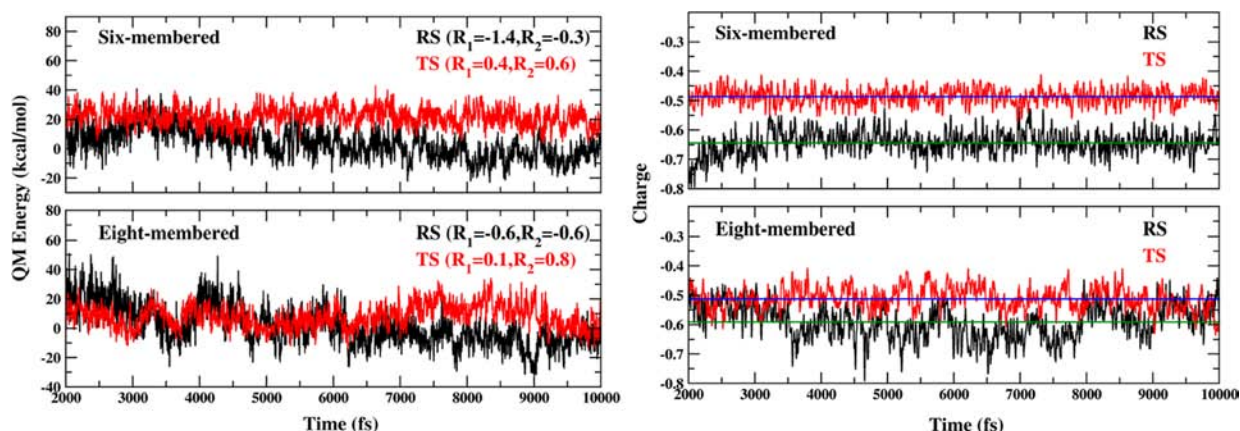


**Figure 5.** The left panels show the calculated QM energy as a function of time for the six- and eight-membered reaction. The QM energy includes the self-energy of QM part and its electrostatic interaction with the RNA/solvent charges. The energy was subtracted by a common constant when plotting. The upper left panel shows the energy of the reactant state (RS) and transition state (TS) for the six-membered reaction. The lower left panel shows the windows in the eight-membered reaction. The right panels show the charge fluctuation of the carbonyl oxygen atom at the reactant state and transition state for the six- and eight-membered reaction. The simulation windows are the same as those in the left panels. The blue and green lines show the average charge of RS and TS.

the reported crystallographic studies which confirmed the presence of some of the water molecules.<sup>6</sup>

**QM Energies and Charge Evolution.** The simulated QM energies were presented in Figure 5 (left panels) for the six- and eight-membered reaction. The energy difference between the transition state and the reactant state is larger for the six-membered reaction than for the eight-membered one. This is consistent with the simulated free energies shown in Figure 2. Indeed the free energy barrier is 10 kcal/mol higher for the six-membered reaction than that for the eight-membered one. These energy curves exhibit fluctuation but overall are flat, which demonstrate that our simulations have reached equilibrium and convergence. The small amplitude fluctuation indicates that the active site of the ribosome is structurally rigid and rationalizes that the reaction entropy change obtained by experimental kinetic measurements is small in the ribosome.<sup>10</sup>

As a major advantage of the *ab initio* QM/MM simulation, it gives us opportunity to investigate the reactions at the electronic level while taking the important electrostatic effect of the environment into account. We can look at the change of the charge distribution of the reacting species during the course of the reaction (of course, under the Born–Oppenheimer approximation). The calculated electrostatic potential (ESP) partial charges of the carbonyl oxygen atom are shown in the right panels of Figure 5. It seems counterintuitive that when the reaction goes from the reactant state to the transition state, the absolute values of the oxygen atom charge actually go down (i.e., become less negative), instead of going up as one would expect. This can be understood as the molecular charge distribution becomes more delocalized when the C–N peptide bond forms (i.e., charges are shared among more atoms). The change for the eight-membered reaction is even smaller (0.1 electron), compared to the six-membered one (0.15 electron), because there is a water molecule hydrogen-bonded to this oxygen atom. Our simulation results corroborate recent experimental results that little stabilization of the carbonyl oxygen was found.<sup>52</sup>

## CONCLUSIONS

The PTC of the large subunit of the ribosome translates the genetic messages carried in tRNA and catalyzes the synthesis of

new proteins. This peptidyl transfer reaction is of fundamental importance in biological functions. Several proposals<sup>6,28,53,54</sup> have been put forward to explore the possible mechanistic routes of this reaction. In this study, we carried out extensive *ab initio* QM/MM MD simulations to characterize the two-dimensional reaction free-energy surface corresponding to two possible reaction mechanisms. The transition states of both the six-membered and eight-membered reactions showed a late TS structure. This late feature of TS is consistent with previous theoretical studies.<sup>22–24,26</sup> In addition, the calculated free-energy barrier of the eight-membered mechanism is 19 kcal/mol, in excellent agreement with the experimental barrier, while the six-membered reaction presented a quite large barrier of 29 kcal/mol. Thus, our simulation results indicate that the eight-membered reaction mechanism associated with much lower free-energy barrier is more favorable for the reaction in the ribosome.

We need to point out that in order to make the computation tractable, not all of the atoms involved in bond-breaking and bond-forming during the reaction are included in the reaction coordinates when scanning the free-energy surfaces. Nevertheless, we believe the conclusions we draw based on the simplified reaction coordinates are robust, since the large free-energy difference from our simulations enables us to discriminate the two proposed reaction mechanisms confidently.

Our simulation results reveal the remarkable functional role played by water molecules in the ribosome active site, and further confirm the energetic advantage when a water acts as a proton shuttle for the multiproton transfer process during the reaction. The delicate interplay between the ribosome and water makes protein synthesis efficient.

## ASSOCIATED CONTENT

### Supporting Information

Simulated reaction structures and complete ref 47. This material is available free of charge via the Internet at <http://pubs.acs.org>.

## ■ AUTHOR INFORMATION

## Corresponding Author

yxjiang@phy.ecnu.edu.cn

## Notes

The authors declare no competing financial interest.

## ■ ACKNOWLEDGMENTS

This work was supported by the National Natural Science Foundation of China (NSFC, Grant Nos. 20903040, 10974054 and 20933002). We thank the supercomputer center at ECNU for computer time.

## ■ REFERENCES

- (1) Schmeing, T. M.; Ramakrishnan, V. *Nature* **2009**, *461*, 1234.
- (2) Leung, E. K. Y.; Suslov, N.; Tuttle, N.; Sengupta, R.; Piccirilli, J. A. *Annu. Rev. Biochem.* **2011**, *80*, 527.
- (3) Ban, N.; Nissen, P.; Hansen, J.; Moore, P. B.; Steitz, T. A. *Science* **2000**, *289*, 905.
- (4) Schluenzen, F.; Tocilj, A.; Zarivach, R.; Harms, J.; Gluehmann, M.; Janell, D.; Bashan, A.; Bartels, H.; Agmon, I.; Franceschi, F.; Yonath, A. *Cell* **2000**, *102*, 615.
- (5) Wimberly, B. T.; Brodersen, D. E.; Clemons, W. M.; Morgan-Warren, R. J.; Carter, A. P.; Vornrhein, C.; Hartsch, T.; Ramakrishnan, V. *Nature* **2000**, *407*, 327.
- (6) Schmeing, T. M.; Huang, K. S.; Kitchen, D. E.; Strobel, S. A.; Steitz, T. A. *Mol. Cell* **2005**, *20*, 437.
- (7) Hiller, D. A.; Singh, V.; Zhong, M. H.; Strobel, S. A. *Nature* **2011**, *476*, 236.
- (8) Kuhlencoetter, S.; Wintermeyer, W.; Rodnina, M. V. *Nature* **2011**, *476*, 351.
- (9) Katunin, V. I.; Muth, G. W.; Strobel, S. A.; Wintermeyer, W.; Rodnina, M. V. *Mol. Cell* **2002**, *10*, 339.
- (10) Sievers, A.; Beringer, M.; Rodnina, M. V.; Wolfenden, R. *Proc. Natl. Acad. Sci. U.S.A.* **2004**, *101*, 12397.
- (11) Youngman, E. M.; Brunelle, J. L.; Kochaniak, A. B.; Green, R. *Cell* **2004**, *117*, 589.
- (12) Brunelle, J. L.; Youngman, E. M.; Sharma, D.; Green, R. *RNA* **2006**, *12*, 33.
- (13) Schroeder, G. K.; Wolfenden, R. *Biochemistry* **2007**, *46*, 4037.
- (14) Johansson, M.; Bouakaz, E.; Lovmar, M.; Ehrenberg, M. *Mol. Cell* **2008**, *30*, 589.
- (15) Wohlgenuth, I.; Brenne, S.; Beringer, M.; Rodnina, M. V. *J. Biol. Chem.* **2008**, *283*, 32229.
- (16) Pavlov, M. Y.; Watts, R. E.; Tan, Z. P.; Cornish, V. W.; Ehrenberg, M.; Forster, A. C. *Proc. Natl. Acad. Sci. U.S.A.* **2009**, *106*, 50.
- (17) Thompson, J.; Kim, D. F.; O'Connor, M.; Lieberman, K. R.; Bayfield, M. A.; Gregory, S. T.; Green, R.; Noller, H. F.; Dahlberg, A. E. *Proc. Natl. Acad. Sci. U.S.A.* **2001**, *98*, 9002.
- (18) Polacek, N.; Gaynor, M.; Yassin, A.; Mankin, A. S. *Nature* **2001**, *411*, 498.
- (19) Beringer, M.; Bruell, C.; Xiong, L. Q.; Pfister, P.; Bieling, P.; Katunin, V. I.; Mankin, A. S.; Bottger, E. C.; Rodnina, M. V. *J. Biol. Chem.* **2005**, *280*, 36065.
- (20) Erlacher, M. D.; Lang, K.; Shankaran, N.; Wotzel, B.; Huttenhofer, A.; Micura, R.; Mankin, A. S.; Polacek, N. *Nucleic Acids Res.* **2005**, *33*, 1618.
- (21) Lang, K.; Erlacher, M.; Wilson, D. N.; Micura, R.; Polacek, N. *Chem. Biol.* **2008**, *15*, 485.
- (22) Sharma, P. K.; Xiang, Y.; Kato, M.; Warshel, A. *Biochemistry* **2005**, *44*, 11307.
- (23) Trobro, S.; Aqvist, J. *Proc. Natl. Acad. Sci. U.S.A.* **2005**, *102*, 12395.
- (24) Trobro, S.; Aqvist, J. *Biochemistry* **2006**, *45*, 7049.
- (25) Trobro, S.; Aqvist, J. *Biochemistry* **2008**, *47*, 4898.
- (26) Wallin, G.; Aqvist, J. *Proc. Natl. Acad. Sci. U.S.A.* **2010**, *107*, 1888.
- (27) Acosta-Silva, C.; Bertran, J.; Branchadell, V.; Oliva, A. *J. Am. Chem. Soc.* **2012**, *134*, 5817.
- (28) Dorner, S.; Polacek, N.; Schulmeister, U.; Panuschka, C.; Barta, A. *Biochem. Soc. Trans.* **2002**, *30*, 1131.
- (29) Dorner, S.; Panuschka, C.; Schmid, W.; Barta, A. *Nucleic Acids Res.* **2003**, *31*, 6536.
- (30) Weinger, J. S.; Parnell, K. M.; Dorner, S.; Green, R.; Strobel, S. A. *Nat. Struct. Mol. Biol.* **2004**, *11*, 1101.
- (31) Beringer, M.; Adio, S.; Wintermeyer, W.; Rodnina, M. *RNA* **2003**, *9*, 919.
- (32) Bieling, P.; Beringer, M.; Adio, S.; Rodnina, M. V. *Nat. Struct. Mol. Biol.* **2006**, *13*, 423.
- (33) Warshel, A.; Levitt, M. *J. Mol. Biol.* **1976**, *106*, 421.
- (34) Field, M. J.; Bash, P. A.; Karplus, M. *J. Comput. Chem.* **1990**, *11*, 700.
- (35) Gao, J. *Reviews in Computational Chemistry*; VCH Publishers: New York, 1995; Vol. 7, p 119.
- (36) Hu, H.; Yang, W. T. *Annu. Rev. Phys. Chem.* **2008**, *59*, 573.
- (37) Riccardi, D.; Schaefer, P.; Yang, Y.; Yu, H. B.; Ghosh, N.; Prat-Resina, X.; Konig, P.; Li, G. H.; Xu, D. G.; Guo, H.; Elstner, M.; Cui, Q. *J. Phys. Chem. B* **2006**, *110*, 6458.
- (38) Zhang, Y. K.; Liu, H. Y.; Yang, W. T. *J. Chem. Phys.* **2000**, *112*, 3483.
- (39) Xiang, Y.; Warshel, A. *J. Phys. Chem. B* **2008**, *112*, 1007.
- (40) Friesner, R. A.; Guallar, V. *Annu. Rev. Phys. Chem.* **2005**, *56*, 389.
- (41) Chandra Singh, U.; Kollman, P. A. *J. Comput. Chem.* **1986**, *7*, 718.
- (42) Bakowies, D.; Thiel, W. *J. Phys. Chem.* **1996**, *100*, 10580.
- (43) Rod, T. H.; Ryde, U. *Phys. Rev. Lett.* **2005**, *94*, 138302.
- (44) King, G.; Warshel, A. *J. Chem. Phys.* **1989**, *91*, 3647.
- (45) Lee, F. S.; Warshel, A. *J. Chem. Phys.* **1992**, *97*, 3100.
- (46) Lee, F. S.; Zhen Tao, C.; Warshel, A. *J. Comput. Chem.* **1993**, *14*, 161.
- (47) Frisch, M. J.; G. W. T., Schlegel, H. B. et al. *Gaussian 09*, Revision B.01; Gaussian, Inc.; Wallingford, CT, 2010.
- (48) Becke, A. D. *J. Chem. Phys.* **1993**, *98*, 5648.
- (49) Lee, C. T.; Yang, W. T.; Parr, R. G. *Phys. Rev. B* **1988**, *37*, 785.
- (50) Xiang, Y.; Duan, L.; Zhang, J. Z. H. *J. Chem. Phys.* **2011**, *134*, 205101.
- (51) Kumar, S.; Bouzida, D.; Swendsen, R. H.; Kollman, P. A.; Rosenberg, J. M. *J. Comput. Chem.* **1992**, *13*, 1011.
- (52) Carrasco, N.; Hiller, D. A.; Strobel, S. A. *Biochemistry* **2011**, *50*, 10491.
- (53) Rangelov, M. A.; Vayssilov, G. N.; Yomtova, V. M.; Petkov, D. D. *J. Am. Chem. Soc.* **2006**, *128*, 4964.
- (54) Gindulyte, A.; Bashan, A.; Agmon, I.; Massa, L.; Yonath, A.; Karel, J. *Proc. Natl. Acad. Sci. U.S.A.* **2006**, *103*, 13327.